ISSN 1330-3651 (Print), ISSN 1848-6339 (Online)
https://doi.org/10.17559/TV-20220425205603
Original scientific paper

Influential Factors in the Loading of the Axial Bearing of the Slewing Platform Drive in Hydraulic Excavators

Vesna JOVANOVIĆ, Dragan MARINKOVIĆ*, Dragoslav JANOŠEVIĆ, Nikola PETROVIĆ

Abstract: The paper contains the results of the analysis of factors that influence the loading of the axial bearing of the slewing platform drive mechanism in hydraulic excavators. The following influential factors are considered: the operations of the excavator manipulation tasks, the number of drives in the slewing platform mechanism, and the configuration of the excavator kinematic chain. The importance of the influence of these factors is assessed on the basis of the comparison between certain equivalent loads of the platform drive bearing with the diagrams of allowed load capacities of available bearings. The equivalent loads of the platform drive mechanism bearing are determined using the approach of static and dynamic excavator simulation in the programs developed on the basis of the defined mathematical models of the excavator. The equivalent loads are given with regard to the duration of the manipulation task and in the form of a spectrum of equivalent loads determined in the entire operating area of the excavator. The analysis is performed for three different configurations of the kinematic chain of a tracked hydraulic excavator with the mass of around 100000 kg.

Keywords: axial bearing; hydraulic excavators; slewing platform drive

1 INTRODUCTION

Hydraulic excavators belong to the group of mobile machines whose primary function is the cyclic transport of various materials in a specific working space. Hydraulic excavators perform different functions using the general configuration of the kinematic chain that comprises: the support and movement mechanism L_1, Fig. 1a, the slewing platform L_2 and the manipulator with the boom L_3, stick L_4 and bucket L_5. The spatial manipulation of the excavator is enabled by the kinematic pair consisting of the support and movement mechanism and the slewing platform, connected using a slewing joint in the form of an axial bearing that allows the unlimited rotation of the platform, in both directions, around the vertical axis of the joint. The general model of the platform drive comprises: the hydrostatic part - a hydraulic pump 2.1, Fig. 1b and a hydraulic motor 2.3, connected in an open or closed hydraulic circuit, and the mechanical part - a reducer 2.4 with a gear on the output [1] shaft coupled with a toothed rim of the axial bearing 2.5. Depending on the excavator size, the concept of the slewing platform mechanism can have one or multiple identical drives, Fig. 1c.

The research related to the rotation drive mechanism of the excavator platform mainly deals with: a) loading of large-diameter axial bearings and fatigue analysis of bearing [2-6], b) loading of the track for rolling elements of axial bearings [7-10], c) examination of influential factors for determining bearing load capacity diagrams, which are used, in comparison with equivalent loads, to carry out the selection of axial bearings [11-15], d) loading of the screw joint of axial bearings [16-20], e) hybrid drive mechanisms of the excavator slewing platform [21-25], and f) recovery of the energy generated when the platform stops turning [26-30]. Hydraulic excavators are characterized by a large number of different size models. Furthermore, every excavator model can have various configurations of the kinematic chain with different variants of the movement mechanism Fig. 1a, different types and configurations of the manipulator, as well as a number of tools for performing all sorts of functions in the working space. At that, for all the possible different configurations of the excavator model, the drive mechanism of the slewing platform remains the same. The stated differences imply the complexity of the slewing platform synthesis procedure in designing hydraulic excavators. According to the developed methodology, for the synthesis of the slewing platform drive mechanism it is necessary to first determine the parameters of the kinematic chain members and the parameters of the excavator manipulator drive mechanisms [31, 32].

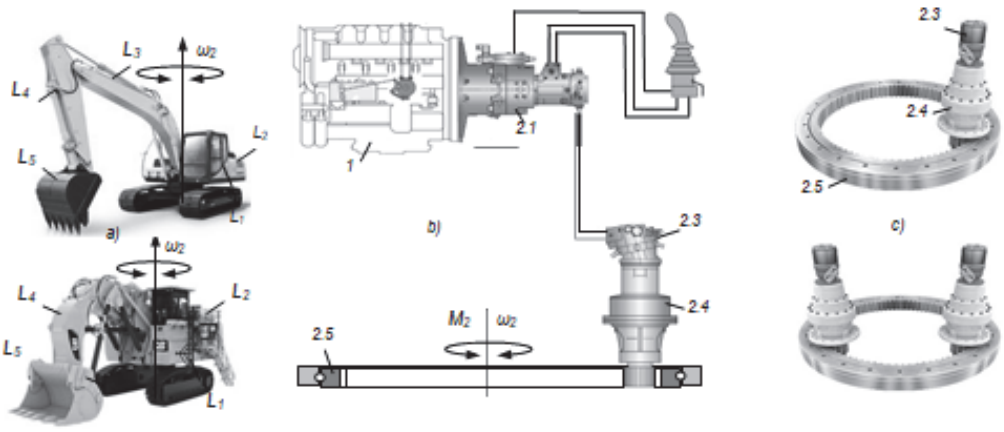

Figure 1 The general concept of the slewing platform drive mechanism in hydraulic excavators: a) kinematic chains of the excavator; b) functional schematic; c) physical models of the drive mechanism

In the initial phase of the synthesis procedure for the slewing platform mechanism, the axial bearing of the drive is the first to be determined. For the proper selection of the size, manner of installation and maintenance of the axial bearing, specialized manufacturers of available bearing models set out certain limitations, criteria and conditions [33-35]. The basic limitation in choosing the axial bearing relates to the allowed load capacity of the bearing given in the form of a bearing load capacity diagram that represents the dependence between the allowed force and the allowed moment of the bearing load. The bearing size is chosen by comparing the bearing load capacity diagrams with equivalent bearing loads determined in line with the criteria defined by bearing manufacturers on the basis of forces and moments to which the bearing is subjected during the operation of the excavator. In what follows, the paper will provide the results of the research into the influence on the loading of the axial bearing of the slewing platform mechanism in hydraulic excavators exerted by the following factors: operations of manipulation tasks, the number of drives in the excavator slewing platform mechanism, and the configuration of the excavator kinematic chain.

2 MATHEMATICAL MODEL OF THE EXCAVATOR

A general mathematical model of the excavator is developed using Newton-Euler dynamic equations [31, 36] for the analysis of the factors that influence the loading of the axial bearing of the slewing platform mechanism. The mathematical model of the excavator encompasses the configuration of the excavator kinematic chain with a loading (Fig. 2a) and a digging (Fig. 2b) manipulator comprising: the tracked support and movement member L_1 (Fig. 2) the slewing member - slewing platform L_2 and the planar manipulator with the boom L_3, stick L_4 and bucket L_5. The members of the excavator kinematic chain form kinematic pairs of the fifth class - slewing joints with one degree of freedom. The center of joint O_2 of the kinematic pair that consists of the support and movement member and the slewing member is the point of intersection of the joint vertical axis and the horizontal plane defined by the centers of the rolling bodies of the axial bearing that connect the support and movement member to the slewing member of the chain. The manipulator drive mechanisms are planar lever configurations with actuators - hydraulic two-way cylinders c_i connected, directly or indirectly, to the members of the kinematic pair L_{i-1} - L_i of the manipulator. The assumptions of the general mathematical model of the excavator are:

- the support surface and the members of the excavator kinematic chain are modeled using rigid bodies;
- during the manipulation task the excavator is subjected to external (technological) load - the digging resistance force $\boldsymbol{W}$, internal load - forces of gravity (weight), and inertia forces and moments of the kinematic chain members, drive mechanisms and material scooped by the excavator bucket;
- hydraulic cylinders of the drive mechanisms are modeled as rods with equally distributed mass along the current length;
- friction is neglected in the joints of the kinematic chain and excavator drive mechanisms, as well as the influence of wind on the members of the excavator kinematic chain;
- the vector of the digging resistance force $\boldsymbol{W}$ acts on the cutting edge of the bucket in point O_w eccentrically displaced in relation to the bucket plane for coordinate z_{5w}.

The eccentric action of the digging resistance force occurs when capturing inhomogeneous material, widening canals, plucking various vegetation and lifting loads.

The space of the excavator model is determined with an absolute coordinate system *OXYZ* (Fig. 2) with unit vectors *i*, *j*, *k* in the direction and sense of coordinate axes *OX, OY* and *OZ*. Each member of the excavator kinematic chain L_i is determined in its own local coordinate system $O_ix_iy_iz_i$ with a set of quantities (marked with a circumflex above the symbol), (Fig. 2) [32, 37]:

$$L_i = \left\{ \hat{\boldsymbol{e}}_i, \hat{\boldsymbol{s}}_i, \hat{\boldsymbol{t}}_i, m_i, \hat{J}_i \right\} \quad \forall\, i = 1,...,5 \tag{1}$$

where: $\hat{\boldsymbol{e}}_i$ - the unit vector (ort) of the axis of the O_i joint that links member L_i to the previous member L_{i-1}; $\hat{\boldsymbol{s}}_i$ - the vector of the position of the O_{i+1} joint center that links member L_i to the following member L_{i+1}, where the vector intensity represents the kinematic length of member L_i; $\hat{\boldsymbol{t}}_i$ - the vector of the position of the mass m_i center of member L_i; $\hat{J}_i$ - the moments of member L_i inertia.

The manipulator drive mechanism C_i in the mathematical model of the excavator is determined in its own local coordinate system $O_{cbi}x_{ci}y_{ci}z_{ci}$ using a set of quantities (Fig. 2):

$$C_i = \left\{ \hat{\boldsymbol{e}}_{ci}, D_i, d_i, m_{ci}, n_{ci}, \hat{\boldsymbol{a}}_i, \hat{\boldsymbol{b}}_i \right\} \quad \forall\, i = 3,...,5 \tag{2}$$

where: $\hat{\boldsymbol{e}}_{ci}$ - the unit vector of the axis of joint O_{cbi} in which the hydraulic cylinder is connected to the manipulator kinematic chain member, D_i/d_i - the diameter of the piston/piston rod in the hydraulic cylinder; m_{ci} - the mass of the hydraulic cylinder; n_{ci} - the number of the hydraulic cylinders in the drive mechanism, $\hat{\boldsymbol{a}}_i, \hat{\boldsymbol{b}}_i$ - the vectors, i.e. coordinates, of the position of the centers of the joints in which the hydraulic cylinders and transmission levers are connected to the members of the drive mechanism kinematic pair.

Generalized coordinates - angles θ_l determine the relative position of member L_i in relation to the previous member L_{i-1} [38]. The position of member L_i in the manipulator kinematic chain is determined in relation to the horizontal absolute plane *XOZ* using angles φ_i (external coordinates):

$$\phi_i = \sum_{i=3}^{i} \theta_i \quad \forall\, i = 3,...,5 \tag{3}$$

The vectors of the positions of joints $\boldsymbol{r}_i$ centers, the centers of masses $\boldsymbol{r}_{ti}$ of the members of the excavator kinematic chain, and the vector of the position of the attacking point of the digging resistance force on the cutting edge of the bucket $\boldsymbol{r}_w$ in relation to the absolute coordinate system are determined using the equations:

$$r_1 = 0, \qquad \boldsymbol{r_i} = \sum_{j=1}^{i-1} A_{jo}\hat{s}_j, \quad r_{\boldsymbol{w}} = \sum_{j=1}^{5} A_{jo}\hat{s}_j, \quad \boldsymbol{r_{ti}} = r_i + A_{io}\hat{t}_i \qquad (4)$$
$$\forall\, i = 2,...,5$$

where: A_{jo}, A_{io} - the transformation matrices of the excavator model used to translate the vector quantities from the local coordinate system of the chain member L_i to the absolute coordinate system of the excavator model, while matrices $A_{oi} = A_{io}^T$ are used vice versa from the absolute to the local coordinate system.

3 EQUIVALENT LOADS OF THE AXIAL BEARING

By fictively breaking the excavator kinematic chain in the center of joint O_2, and observing the balance of the discarded part of the chain (platform and manipulator), one can determine the resulting force $\boldsymbol{F}_{O2}$ and moment $\boldsymbol{M}_{O2}$ in the center of joint O_2 using the equations Fig. 2a, b:

$$\boldsymbol{F}_{O2} = \sum_{i=2}^{5} \boldsymbol{F}_{ui} + \sum_{i=3}^{5} \boldsymbol{F}_{cui} + \boldsymbol{W} \qquad (5)$$

$$\boldsymbol{M}_{O2} = \sum_{i=2}^{5} \boldsymbol{M}_i + \sum_{i=3}^{5} \boldsymbol{M}_{ci} + \sum_{i=2}^{5} \boldsymbol{M}_{Fui} + \sum_{i=3}^{5} \boldsymbol{M}_{Fcui} + \boldsymbol{M}_w \qquad (6)$$

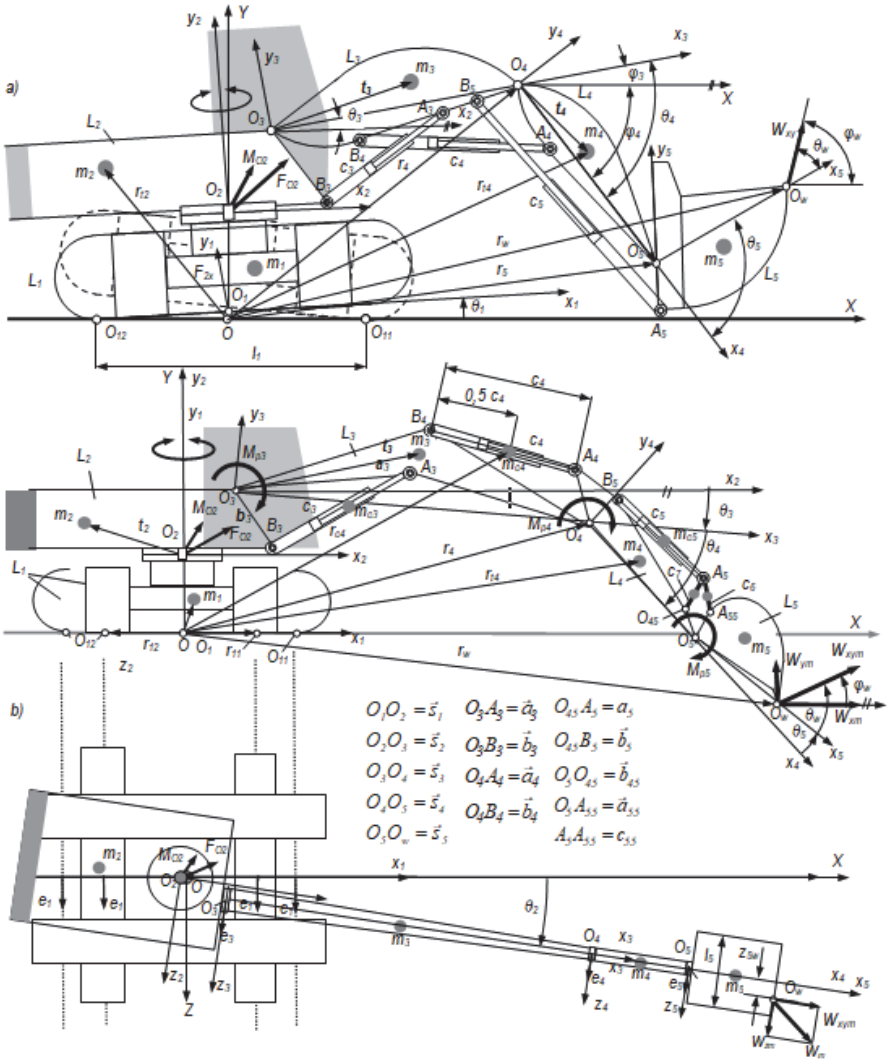

Figure 2 The mathematical model of the excavator with a a) loading and b) digging manipulator

where: $\boldsymbol{F}_{ui}$, $\boldsymbol{F}_{cui}$ - the internal force (inertia and gravity) in the center of mass of the kinematic chain member and actuators (hydraulic cylinders) of drive mechanisms, $\boldsymbol{M}_i$, $\boldsymbol{M}_{ci}$ - the inertia moment in the center of mass of the kinematic chain member and mass of the drive mechanism actuators, $\boldsymbol{M}_{Fui}$, $\boldsymbol{M}_{Fcui}$ - the moment of the internal force of the kinematic chain member and drive mechanism actuators for the center of joint O_2, $\boldsymbol{W}$, $\boldsymbol{M}_w$ - the digging resistance force and the digging resistance force moment for the center of joint O_2. Depending on the number of platform drives and their distribution in relation to the toothed rim of the axial bearing, additional loads of the axial bearing may appear due to the reaction of the platform drive subjected to the action of the loads occurring during the manipulation task of the excavator.

Considering this additional load appearing due to the reaction of the slewing platform drive, resultant $\boldsymbol{F_2}$ and components F_{2x}, F_{2y}, F_{2z} of the force in joint O_2 of the slewing platform that act on the axial bearing of the slewing drive are determined using the equations (Fig. 3a, c):

$$\boldsymbol{F}_2 = \boldsymbol{F}_{O2} + \boldsymbol{F}_{c2},$$
$$\boldsymbol{M}_{O2} = \sum_{i=2}^{5} \boldsymbol{M}_i + \sum_{i=3}^{5} \boldsymbol{M}_{ci} + \sum_{i=2}^{5} \boldsymbol{M}_{Fui} + \sum_{i=3}^{5} \boldsymbol{M}_{Fcui} + \boldsymbol{M}_w \quad (7)$$

where: $\boldsymbol{F}_{c2}$ - the vector of the reaction of the slewing platform drive determined by the equation:

$$\boldsymbol{F}_{c2} = \frac{|M_{p2}|}{D_{25} - d_{24}} \left[\sin(\theta_2 + \alpha_2)\boldsymbol{i} - \cos(\theta_2 + \alpha_2)\boldsymbol{k} \right] \quad (8)$$

where: M_{p2} - the moment of the slewing platform drive, α_2 - the angle of the platform drive position, D_{25} - the pitch diameter of the toothed rim of the platform axial bearing, d_{24} - the pitch diameter of the gear on the output shaft of the drive reducer. The resulting force $\boldsymbol{F}_2$ loads the axial bearing with the radial force $\boldsymbol{F}_{2r}$ that is formed, in the horizontal plane of the bearing, by components $\boldsymbol{F}_{2x}$ and $\boldsymbol{F}_{2z}$, and the axial force $\boldsymbol{F}_{2a}$ that acts along the bearing axis O_{2y} and is equal to component $\boldsymbol{F}_{2y}$. In larger excavators with two identical drives positioned under the angle of $\alpha_2 = 180°$, (Fig. 3d), reactive forces of platform drives cancel each other and do not load the bearing.

Resultant $\boldsymbol{M}_2$ and components M_{2x}, M_{2y} and M_{2z} of moments in joint O_2 of the slewing platform that load the axial bearing of the slewing drive are determined using the equations (Fig. 3b, d):

$$\boldsymbol{M}_2 = \boldsymbol{M}_{O2} - \mathrm{M}_{p2}\boldsymbol{j}_2$$
$$\boldsymbol{M}_{2x} = \boldsymbol{M}_2 \cdot \boldsymbol{i}_2, \quad \boldsymbol{M}_{2y} = \boldsymbol{M}_2 \cdot \boldsymbol{j}_2, \quad \boldsymbol{M}_{2z} = \boldsymbol{M}_2 \cdot \boldsymbol{k}_2 \quad (9)$$

The resulting moment $\boldsymbol{M}_2$ loads the axial bearing with moment $\boldsymbol{M}_{2r}$ consisting of components $\boldsymbol{M}_{2x}$ and $\boldsymbol{M}_{2z}$, whose vector lies in the horizontal plane of the bearing. Component $\boldsymbol{M}_{2y} = 0$ does not load the bearing, since the loading moment component M_{O2y} and the drive moment M_{p2} have the same intensity and the opposite direction of action.

As suggested by manufacturers, the size of the axial bearing of the slewing platform mechanism in mobile machines is selected based on the equivalent bearing loads. The diagram of the allowed bearing load capacity that shows the dependence of the allowed equivalent force F_e and the allowed equivalent moment M_e of the bearing defined by the equations [39] is used for this purpose:

- for the equivalent force:

$$F_e = (a \cdot F_{2a} + b \cdot F_{2r}) \cdot f_s \quad (10)$$

- for the equivalent moment:

$$M_e = c \cdot M_{2r} \cdot f_s \quad (11)$$

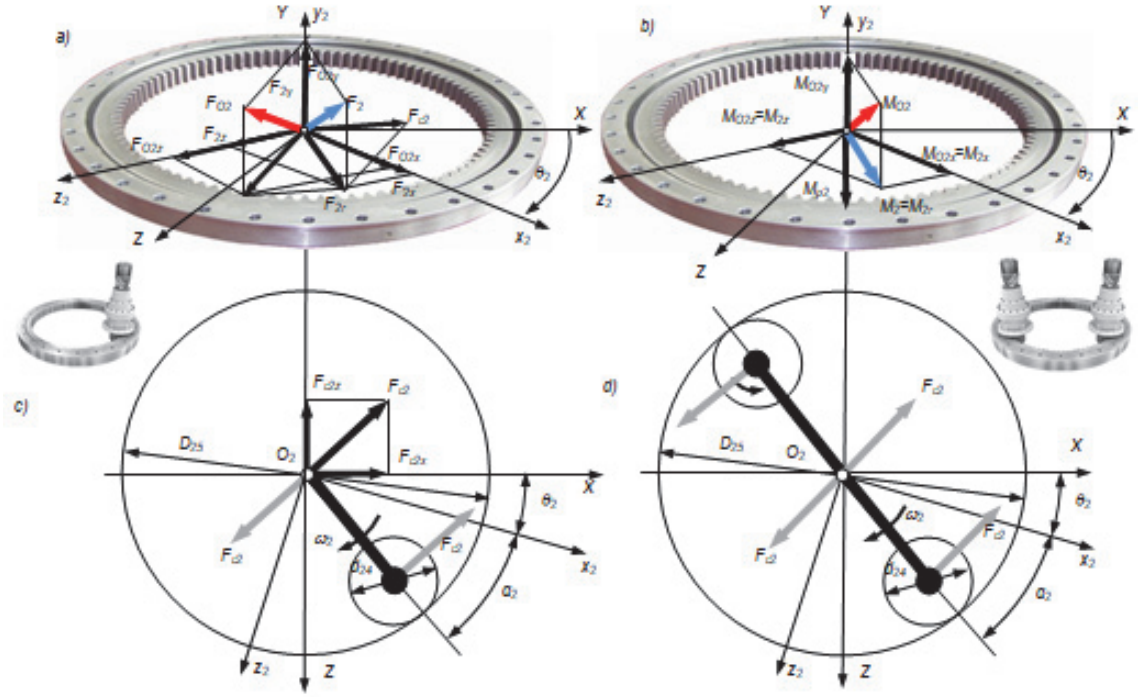

Figure 3 Components of the loading of the axial bearing of the excavator slewing platform drive: a) forces; b) moments; c) bearing loading forces with one drive; d) bearing loading forces with two drives

where: F_{2a}, F_{2r} - the axial and radial bearing load force, M_{2r} - the bearing load moment, a, b, c - the coefficients dependent on the type of bearing, type and size of the machine and its working conditions, f_s - the factor of static safety. When choosing a bearing, the condition is that the values of the calculated equivalent bearing loads in the entire operating area of the machine do not exceed the boundary curves in the bearing load capacity diagram.

4 INFLUENTIAL FACTORS IN THE LOADING OF THE AXIAL BEARING

The factors that influence the loading of the axial bearing of the slewing platform drive were analyzed for three possible variants A, B and C of the same hydraulic excavator model (Tab. 1) with the mass of around 100000 kg. The variants have different members of the

kinematic chain with the same slewing platform mechanism with two drives positioned relatively at the angles: $\alpha_2 = 0°$ and $\alpha_2 = 180°$ (Fig. 3c, d) along the circumference of the toothed rim of the axial bearing. The excavator variants *A* and *B* possess different support and movement mechanisms and loading manipulators with different bucket volumes. Excavator variant *A* has the bucket volume of $V = 4.4$ m^3 for digging the material with the density of $\rho = 2200$ kg/m^3, while variant *B* has the bucket volume of $V = 6.5$ m^3 for digging the material with the density of $\rho = 1650$ kg/m^3. Variant *C* has a digging manipulator with the bucket volume of $V = 4.8$ m^3 for digging the material with the density of $\rho = 2200$ kg/m^3.

The importance of the influence of specific factors on the loading of the slewing platform drive bearing is assessed by comparing the calculated equivalent loads of excavator variants *A, B* and *C* bearings with the allowed loads - the diagram of load capacity of different available single-line roller bearings *AL0-AL6* (Tab. 2) [37].

4.1 Analysis of the Influence of Manipulation Task Operations

Based on the defined mathematical model of the excavator and the developed program, static and dynamic numerical simulation of the excavator operation were performed to analyze the influence of the manipulation task operations for the loading of the axial bearing of the excavator slewing platform drive. The manipulation task parameters were set for the following operations: digging, transferring, unloading and returning to the new digging plane. The simulation was used to determine the change in equivalent forces and equivalent moments of the loading of the axial bearing in the slewing platform drive mechanism of the excavator variants *A* and *B* with the loading manipulator depending on the duration of the manipulation task. Dynamic parameters of the excavator kinematic chain members L_i and drive mechanisms C_i, used in simulating the excavator variants *A*, *B* and *C* were determined using the developed *3D* excavator models that correspond to the physical model of the Liebherr R974C Litronic hydraulic excavator. *SolidWorks* software [40] was used for the purpose.

Simulated components of the digging resistance force ***W*** (Fig. 4), that load the kinematic chain of excavator variants *A* and *B* were defined using analytical mathematical models depending on the bucket geometry, changes in the cutting thickness and characteristics of the material scooped during the digging operation [31].

Digging resistance force components perpendicular (W_{xy}) and colinear (W_z) in relation to the cutting edge of the excavator variant *A* and *B* buckets have similar intensities and an insignificantly varying character of changes during the digging operation. Conditions for simulating the stable operation of the excavator ($\theta_{11} = 0°$) are met because the intensity of the perpendicular component of the digging resistance W_{xy} is smaller than the intensity of the boundary digging resistance forces W_{sm}, W_{pm} determined from the stability conditions: absence of rolling over (W_{sm}) and sliding (W_{pm}) of the excavator in the support plane.

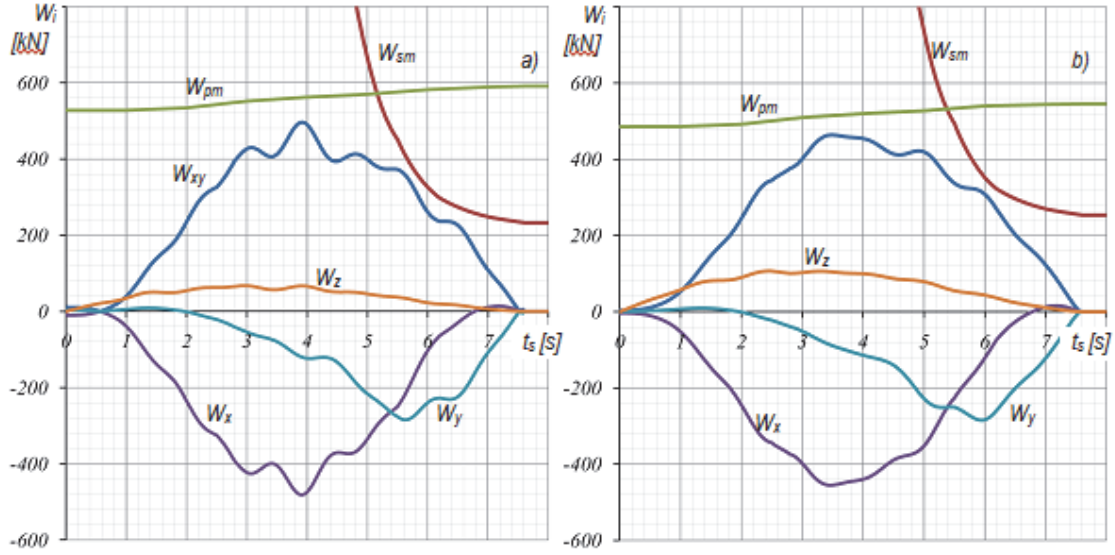

Figure 4 Components of the digging resistance force perpendicular (W_x, W_y, W_{xy}) and colinear (W_z) in relation to the bucket cutting egde and forces (W_{sm}, W_{pm}) allowed by the stability of the excavator model: a) *A*; b) *B*

Table 1 Possible variants of the excavator kinematic chain members [31]

Model	Tracked support and movement mechanism			Manipulator			material density ρ / kg/m^3	excavatormass m / kg
	footprint length L_1 / mm	track span B_1 / mm	tread width b_1 / mm	kinematic chain	bucket volume V / m^3	bucket width b_5 / mm		
A	4770	3600	500	loading	4.4	2350	2200	92000
B	5035	3600	600	loading	6.5	3150	1650	100000
C	4770	3600	500	digging	4.8	2150	2200	89000

Table 2 Single-line roller axial bearings [37]

Bearing mark	*AL0*	*AL1*	*AL2*	*AL3*	*AL4*	*AL5*	*AL6*
Rolling bodies track diameter / mm	2125	2237	2365	2363	2507	2651	2657
Bearing load coefficients	$a = 1$, $b = 2.05$, $c = 1$ $f_s = 1.45$						

In the simulation the vector of the digging resistance force acts upon the cutting edge of the bucket eccentrically in relation to the center of the cutting edge at the distance of $w_{5z} = l_5/4$, one fourth of the bucket width l_5 away (Fig. 2b). For excavator variants *A* and *B*, for the purpose of a comparative analysis, the same working environment parameters and the same working technology model was simulated. Hence, the same manipulation task was performed with the given external cycloid trapezoid model of the character of changes in angular velocities $\dot{\theta}_i$ of the relative movement of the excavator kinematic chain members (Fig. 5) [31]. As simulation results, the diagrams of changes in equivalent static F_{es} and dynamic F_{ed} forces (Fig. 6a) and equivalent static M_{es} and dynamic M_{ed} moments (Fig. 6b) of the axial bearing loading in the slewing platform of excavator variants *A* and *B* are presented.

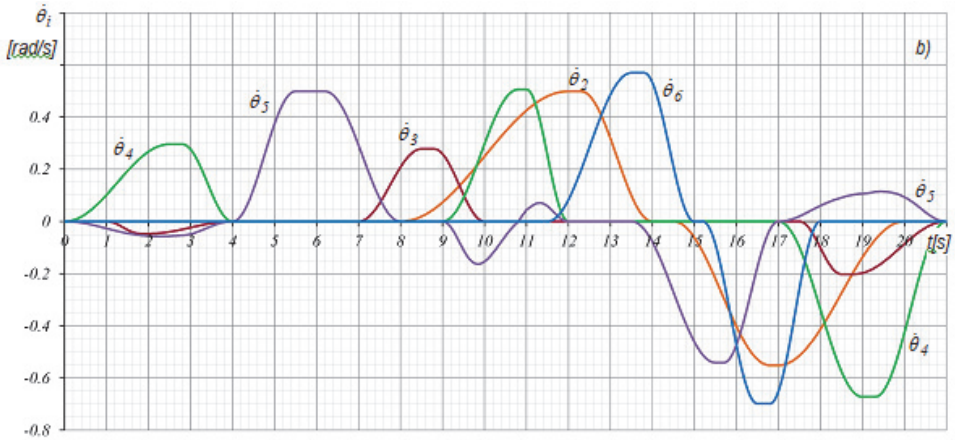

Figure 5 Changes in the angular velocity of relative movement of the kinematic chain members for excavator variants *A* and *B* during the manipulation task

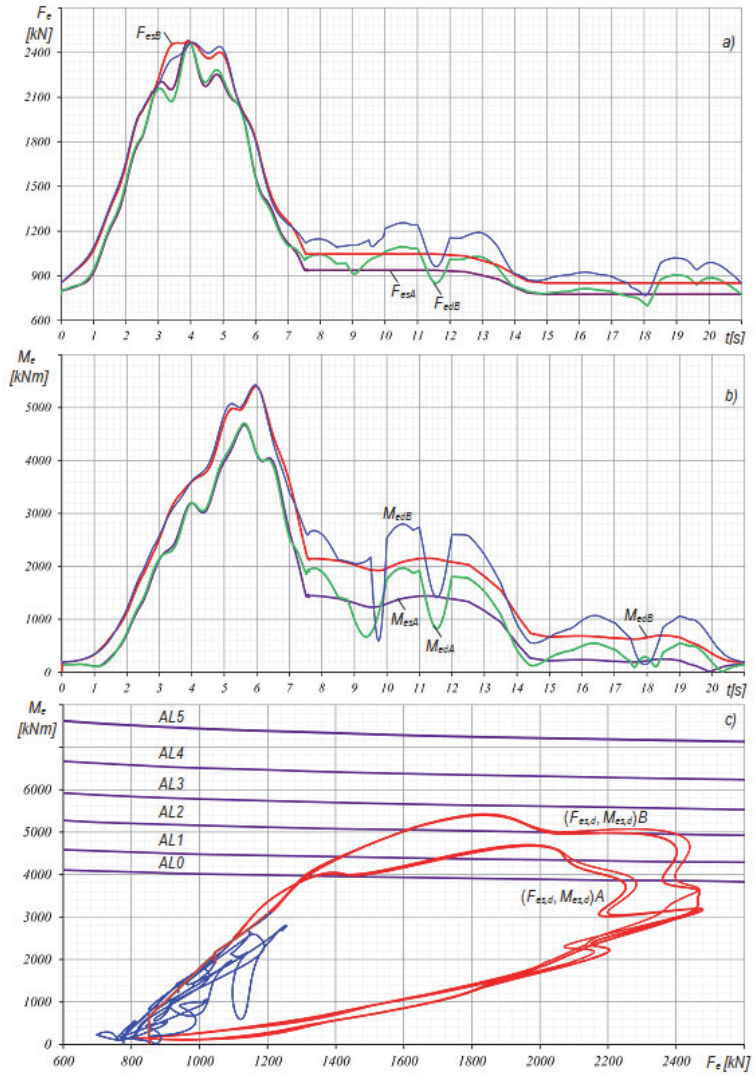

Figure 6 Equivalent loads of the axial bearing of the slewing platform drive in excavator models *A* and *B*: a) equivalent static (F_{es}) and dynamic (F_{ed}) forces; b) equivalent static (M_{es}) and dynamic (M_{ed}) moments; c) equivalent bearing loads in relation to the allowed load capacities of available bearings *AL*0-*AL*5

The results show that the greatest equivalent bearing loads appear during the digging operation. Comparing static and dynamic equivalent loads according to Eq. (5) and Eq. (6), the static bearing loading is subjected to the influence of the digging resistance force and gravity of the kinematic chain members and drive mechanisms, while the inertia loading due to the acceleration of the excavator kinematic chain members during the manipulation task is neglected.

The difference between the dynamic bearing loads and the equivalent static loads during the digging operation is very small, due to the relatively slow movement of the kinematic chain members.

The appearance of greater dynamic loads, which act upon the platform axial bearing, occurs at the beginning and the end of the material transfer operation and the operation of returning to the new digging plane, caused by less and more intense movement of the platform and the manipulator kinematic chain members.

For the sake of comparison, Fig. 6c depicts the allowed load capacities of available bearings *AL*0-*AL*5, while the red line shows the dependence of the equivalent forces and moments of the bearing loads, F_e and M_e, in the excavator variants *A* and *B* during the simulated manipulation task in the digging operation. The blue line is used for other operations.

The diagram shows that the equivalent loads of the axial bearing determined during the digging operation are pertinent for the selection of the bearing size. This is because the flow of changes in the equivalent forces and moments during the digging operation (Fig. 6c, red line) is much closer to the boundary lines of the allowed load capacities of available bearings in relation to the changes in the equivalent bearing loads during other operations of the excavator manipulation task (blue lines).

4.2 Analysis of the Influence of the Number of Platform Drives

To assess the influence of the number of slewing platform drives and their relative installation position on the equivalent loads of the drive axial bearing, the analysis was performed in which the equivalent bearing loads for excavator model *B* variants with one (Fig. 3a, c and two identical drives (Fig. 3b, d) were considered. In excavator variant *B* with one slewing platform drive, the drive was taken to be positioned in the local coordinate system of the platform, with the angles $\alpha_2 = 0^o$, $\alpha_2 = 180°$ in relation to the O_2x_2 axis (Fig. 3a, c). This corresponds to the most common type of installation in practice, bearing in mind the available space and the proximity of the hydraulic motor and the hydraulic pumps of the excavator drive group. In the excavator model variant with two slewing platform drives, the drives were positioned relatively under the angles $\theta_2 = 0^o$, $\alpha_{21} = 0^o$, $\alpha_{22} = 180^o$ (Fig. 3b, d) in the local coordinate system of the platform.

The analysis results obtained by simulation are presented in Fig. 7. The allowed load capacities of available bearings *AL*0-*AL*5 show that, during the digging operation (red line), the dependences between the static and dynamic equivalent bearing loads of excavator variant *B* with one slewing platform drive ($F_{es\mathrm{I}}$, $M_{es\mathrm{I}}$ and $F_{ed\mathrm{I}}$, $M_{ed\mathrm{I}}$) differ from the excavator variant *B* with two slewing platform drives ($F_{es\mathrm{II}}$, $M_{es\mathrm{II}}$ and $F_{ed\mathrm{II}}$, $M_{ed\mathrm{II}}$). It is noticeable that the excavator variant *B* with one slewing platform drive has greater equivalent forces ($F_{s\mathrm{I}}$, $F_{d\mathrm{I}}$) of bearing loads compared to the equivalent forces ($F_{s\mathrm{II}}$, $F_{ed\mathrm{II}}$) of the excavator variant *B* with two drives.

The dependences of the equivalent bearing loads during other operations of the manipulation task (transfer, unloading and returning to the new digging plane - blue line in Fig. 6c) done by the excavator variant *B* with one drive show that the equivalent forces ($F_{s\mathrm{I}}$, $F_{d\mathrm{I}}$) of bearing loads are significantly greater than the same of the excavator variant *B* with two drives (blue line) (Fig. 6c) [31].

The reason behind the increased equivalent forces lies in the fact that in the excavator variant with one drive a reactive turning force appears, causing a further radial loading of the axial bearing. The increased reactive forces in the slewing mechanism with one drive appear during the manipulation task in the digging operation in the case of the eccentric action of the digging resistance force in relation to the longitudinal symmetrical plane of the bucket, i.e. the manipulator, and in the phases of increased and decreased movement of the excavator slewing platform.

In the excavator variant with two drives, the reactive forces of the drive positioned relatively, along the toothed rim of the bearing, at the angle of $\alpha_2 = 180^o$ have the same intensities but opposite directions of action so that they do not subject the axial bearing to further loads. The equivalent moments of bearing loads for both slewing drive variants of excavator variant *B* are identical since the drive reactive forces have no influence on them.

4.3 Analysis of the Influence of the Excavator Kinematic Chain Configuration

Bearing in mind that during their operation hydraulic excavators have a number of manipulation tasks with the digging operation - scooping the material in the entire working space, a spectrum of equivalent bearing loads is used for the analysis of the influence of the excavator kinematic chain configuration on the loading of the axial bearing.

The spectrum of equivalent loads of the axial bearing of the excavator slewing platform drive (Fig. 8) represents a constellation of points defined by the equivalent forces F_e and equivalent moments M_e of bearing loads as coordinates. Those points are determined for each position of the excavator kinematic chain and the direction in which the digging resistance acts.

For a reliable selection of the appropriate size of the axial bearing of the slewing platform drive mechanism in the same excavator model, it is necessary to determine the spectra of bearing loads for all possible configurations of the excavator kinematic chain when performing functions in the entire working space under different working conditions.

The spectrum of equivalent loads of the axial bearing of the slewing platform drive is determined in line with the defined mathematical model of the excavator and based on the set of known parameters [30]:

$$U = \left\{ L_i, C_i, \theta_{wp}, \theta_{wk}, p_{\max}, K_2, n_3, n_4, n_5, n_w \right\} \tag{12}$$

where: L_i - the set of parameters of the excavator kinematic chain members, C_i - the set of parameters of the excavator manipulator drive mechanisms, θ_{wp}/θ_{wk} - the initial/final angle of action of the digging resistance force, $p_{\max}$ - the maximum

pressure of the excavator hydrostatic system, K_2 - the set of coefficients for determining the equivalent loads of the axial bearing, n_3 - the desired number of the manipulator boom positions in its movement range, n_4 - the desired number of the stick positions in its movement range for the specific position of the manipulator boom, n_5 - the desired number of the bucket positions in its movement range for the specific position of the manipulator stick, n_w - the desired number of changes in the direction of the digging resistance force action in the range of changes from θ_{wp} to θ_{wk} for each bucket position.

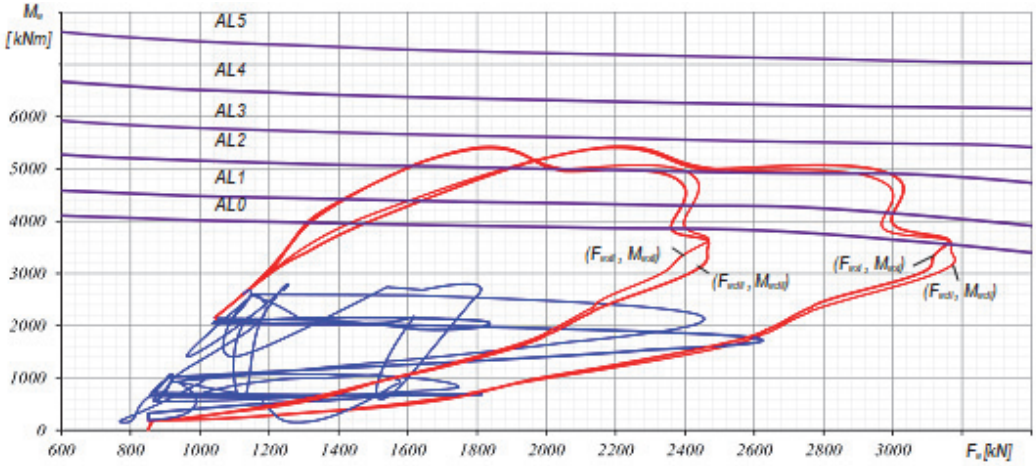

Figure 7 Comparison of equivalent bearing loads of excavator *B* with one (F_{esI}, F_{edI}, M_{esI}, M_{edI}) and two (F_{esII}, F_{edII}, M_{esII}, M_{edII}) platform drives in relation to the allowed load capacities of bearings *AL0*-*AL5*

When determining the spectrum of equivalent loads one takes into account that the loading of the axial bearing is affected by the gravitational forces of the kinematic chain members, the excavator drive mechanisms and the bucket, and the possible digging resistance force W_{xym} defined by the equation (Fig. 2b):

$$W_{xym} = \min\left\{ W_{sm}, W_{pm}, W_{3m}, W_{4m}, W_{5m} \right\} \tag{13}$$

where: W_{pm} - the force of the boundary digging resistance determined from the non-sliding conditions of the excavator in the support surface plane and W_{sm} - the force of the boundary digging resistance determined from the set excavator stability conditions for potential rollover lines, W_{3m}, W_{4m}, W_{5m} - the boundary digging resistance forces limited by the maximal possibilities of the action of the drive mechanisms in the manipulator boom, stick and bucket.

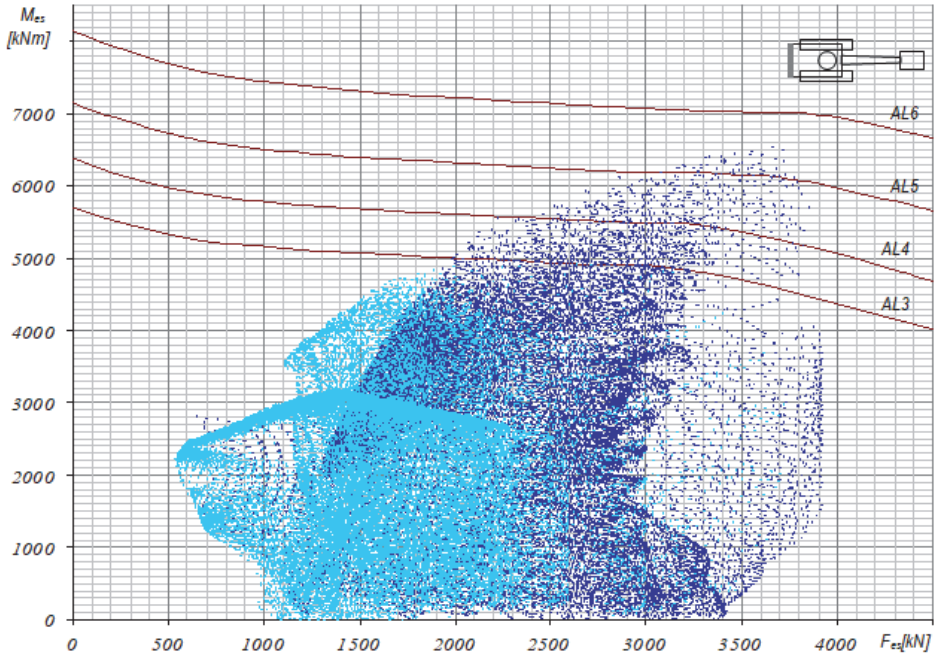

Figure 8 Comparison of the spectra of the axial bearing loads in excavator model *A* with the loading manipulator with the bucket volume $V = 6.5$ m³ (the dark blue color) and excavator mode *C* with the digging manipulator (bright blue) with the bucket volume $V = 4.8$ m³ [30]

An originally developed program based on the presented mathematical model of the excavator was used for the analysis of the influence of changes in the excavator kinematic chain configuration. Fig. 8 shows the obtained spectra of the loading of the slewing platform bearing of excavator variant *A* with the loading manipulator (the dark blue color of the spectrum) and excavator variant *C* with the digging manipulator (the bright blue color of the spectrum). The loading spectra are presented in the diagrams of the allowed load capacity of the selected

available bearings: *AL3*-*AL6*. They are determined according to the following given conditions and parameters: the manipulator is perpendicular to the transversal plane of the support and movement mechanism, positions of the kinematic chain $n_3 = 30$, $n_4 = 20$, $n_5 = 10$; the number of changes in the directions of the digging resistance force action is $n_w = 10$; and the initial/final angle of the direction of the digging resistance force action is $\theta_{wp}/\theta_{wk} = 200°/300°$ for variant *A* and $\theta_{wp}/\theta_{wk} = 30°/50°$ for variant *C*.

Diagram in Fig. 8 shows that the spectra are very different and that the selection of the axial bearing size relies on the spectrum of the equivalent bearing loads of excavator variant *A* with the loading manipulator configuration. This is due to much greater equivalent bearing loads than in the case of the equivalent bearing loads of excavator variant *C* with the digging manipulator. The difference occurs due to the different digging technologies, i.e. different action of the digging resistance force. In the digging manipulator, while digging, which takes place mainly below the excavator support level, the bucket movement kinematics is such that, in the majority of the digging operation, the vertical component of the digging resistance force has an opposite direction to the direction of the gravitational forces of the excavator kinematic chain members. This results in the smaller axial loading force exerted on the bearing of the excavator slewing platform drive. Conversely, in the loading manipulator, the bucket movement kinematics is such that, in the majority of the digging operations, the vertical components of the digging resistance force and the gravitational forces of the kinematic chain members have the same direction of action.

This results in the greater axial bearing force acting onto the axial bearing of the slewing platform drive. The results of the analysis using the loading spectra show (Fig. 8) that for the same excavator model, changes in the configuration, i.e. the kinematic chain members, significantly alter the equivalent loads of the axial bearing of the excavator slewing platform drive mechanism.

5 CONCLUSION

In the synthesis of the drive mechanism of the slewing platform in hydraulic excavators, the axial bearing of the mechanism is determined based on equivalent bearing loads and the allowed bearing load capacity. Equivalent loads - equivalent force and equivalent moment are determined according to the criteria of bearing manufacturers depending on the bearing loads that appear during the excavator operation. It is characteristic of hydraulic excavators that a number of factors influence the loading of the platform drive axial bearing. The paper singled out and analyzed the influential factors that are related to: the operations of the excavator manipulation tasks, the number of the slewing platform drive mechanisms and the configuration of the excavator kinematic chain.

The analysis results, obtained through static and dynamic numerical simulation of the excavator operation - by setting the manipulation task with the following operations: digging, transferring, unloading and returning to the new digging plane, show that the bearing loads in the digging operation are pertinent for the selection of the bearing size. The number of drives in the excavator slewing platform mechanism affects the loading of the axial bearing due to the action of the reactive drive force. In the mechanism with two drives positioned relatively along the circumference of the toothed rim of the axial bearing under the angle of 180°, the reactive drive forces are in balance and do not load the bearing. The obtained results also show that a significant influence on the loading of the slewing platform axial bearing is exerted by the kinematic chain configuration and the excavator working technology. This is emphasized by the example that the bearing loads pertinent for its selection are much greater when the excavator is equipped with the loading instead of the digging manipulator.

The general conclusion from the conducted research is that the choice of an axial bearing for the slewing platform mechanism must account for the analyzed influential factors that affect the loading of the axial bearing. This is because the same excavator model can have different configurations of its kinematic chain used to perform a number of different functions.

Based on the axial bearing load spectrum for the entire working area of the excavator, future research can determine the cumulative loads for the analysis of the reliability and service life of the axial bearing.

Acknowledgements

This research was financially supported by the Ministry of Education, Science and Technological Development of the Republic of Serbia (Contract No. 451-03-9/2021-14/200109).

6 REFERENCES

[1] Smajic, J., Saric, I., Muminovic, A., Delic, M., & Muminovic, J. A. (2021). Planetary Gearbox Prototype Development and Manufacturing. *Tehnički Glasnik*, *15*(4), 534-540. https://doi.org/10.31803/tg-20210219170243

[2] Heras, I., Aguirrebeitia, J., Abasolo, M., Coria, I., & Escanciano, I. (2019).Load distribution and friction torque in four-point contact slewing bearings considering manufacturing errors and ring flexibility. *Mechanism and Machine Theory*, *137*, 23-36. https://doi.org/10.1016/j.mechmachtheory.2019.03.008

[3] Maheedhara Reddy, G., Diwakar Reddy, V., Satheesh Kumar, B., & Shyamsunder, J. (2018). Experimental investigation on radial ball bearing parameters using Taguchi method. *Journal of Applied and Computational Mechanics*, *4*(1), 69-74. https://doi.org/10.1080/01430750.2019.1611635

[4] Junning, L., Ka, H., Qian, W., Wuge, C., & Jiafan, X. (2022). Thermal elastohydrodynamic lubrication analysis of high-speed and light-load rolling bearing with double rings rotation. *Technical Gazette*, *29*(1), 30-37. https://doi.org/10.17559/TV-20200210192943

[5] Yao, C. (2022). Diagnosis of Bearing Damage in Mechanical Equipment Combining Fuzzy Logic Variable Phase Layered Algorithm. *Technical Gazette*, *29*(2), 379-385. https://doi.org/10.17559/TV-20210413082734

[6] Jovanović, V., Janošević, D., & Pavlović, J. (2021). Analysis of the influence of the digging position on the loading of the axial bearing of slewing platform drive mechanisms in hydraulic excavators. *Facta Universitatis-Series Mechanical Engineering*, *19*(4), 705-718. https://doi.org/10.22190/FUME190225020J

[7] Kania, L., Pytlarz, R., & Spiewak, S. (2018). Modification of the raceway profile of a single-row ball slewing bearing. *Mechanism and Machine Theory*, *128*, 1-15.

https://doi.org/10.1016/j.mechmachtheory.2018.05.009
[8] Potočnik, R., Flašker, J., & Glodež, S. (2009). Fatigue analysis of large slewing bearing using strain - life approach. *12th International Conference on Fracture, ICF12.*
[9] Knuth, J. A. (2013). *Rolling contact fatigue of low hardness steel for slewing ring application*. Master thesis, The University of Wisconsin-Milwaukee.
[10] Krynke, M., Selejdak, J., & Borkowski, S. (2012). The quality of materials applied for slewing bearing raceway, technical paper. *Materials Engineering - Materiálové inžinierstvo*, *19*, 157-163. https://doi.org/10.1007/s12206-011-1203-4
[11] Qiu, M., Yan, J., Zhao, B., Chen, L., & Bai, Y. (2012). A finite element analysis of the connecting bolts of slewing bearings based on the orthogonal method. *Journal of Mechanical Science and Technology*, *26*(3), 883-887.
[12] Krynke1, M., Selejda, J., & Borkowski, S. (2013). Determination of static limiting load curves for slewing bearing with application of the finite element method. *Materials Engineering - Materiálové inžinierstvo*, *20*, 64-70.
[13] Potočnik, R., Göncz, P., & Glodež, S. (2013). Static capacity of a large double row slewing ball bearing with predefined irregular geometry. *Mechanism and Machine Theory*, *64*, 67-79. https://doi.org/10.1016/j.mechmachtheory.2013.01.010
[14] Kania, L. (2005). *Analysis of internal load of slewing bearings in respect of their load carrying capacity.* Wyd. Politechniki Częstochowskiej, Częstochowa.
[15] Wang, Y. & Yuan, Q. (2014). Static load-carrying capacity and fatigue life of a double row pitch bearing with radial interference. *The Journal of Mechanical Engineering Science*, *228*(2), 307-316. https://doi.org/10.1177/0954406213486042
[16] Qiu, M., Yan, J., Zhao, B., Chen, L., & Bai, Y. (2012). A finite element analysis of the connecting bolts of slewing bearings based on the orthogonal method. *Journal of Mechanical Science and Technology*, *26*(3), 883-887. https://doi.org/10.1007/s12206-011-1203-4
[17] Göncz, P. & Glodež, S. (2009). Calculation model for pre-stressed bolted joints of slewing bearings. *Advanced Engineering*, *2*(3), 175-186.
[18] Reszka, P., Kania, L., & Pytlarz, R. (2012). Numerical analysis of the screw connection with preload tension used in the mounting of slewing bearings. *Journal of KONES Powertrain and Transport*, *19*(2), 465-472. https://doi.org/10.5604/12314005.1138249
[19] Hossain, J. (2014). *Effects of Pretension in Bolt for a Slewing Bearing*. Master thesis, Norwegian University of Science and Technology Department of Marine Technology.
[20] Chaib, Z., Daidié, A. & Leray, D. (2007). Screw behavior in large diameter slewing bearing assemblies: numerical and experimental analyses. *International Journal on Interactive Design and Manufacturing*, *1*(1), 21-31. https://doi.org/10.1007/s12008-007-0003-7
[21] Wang, D., Guan, C., Pan, S., Zhang, M., & Lin, X. (2009). Performance analysis of hydraulic excavator powertrain hybridization. *Journal Automation in Construction*, *18*(3), 249-257. https://doi.org/10.1016/j.autcon.2008.10.001
[22] Lin, T., Wang, Q., Hu, B., & Gong, W. (2010). Development of hybrid powered hydraulic construction machinery. *Journal Automation in Construction*, *19*(1), 11-19. https://doi.org/10.1016/j.autcon.2009.09.005
[23] Hui, S. & Junqing, J. (2010). Research on the system configuration and energy control strategy for parallel hydraulic hybrid loader. *Journal Automation in Construction*, *19*(2), 213-220. https://doi.org/10.1016/j.autcon.2009.10.006
[24] Xiao, Q., Wang, Q., & Zhang, Y. (2008). Control strategies of power system in hybrid hydraulic excavator. *Journal Automation in Construction*, *17I*(4), 361-367. https://doi.org/10.1016/j.autcon.2007.05.014
[25] Kagoshima, M. (2013). The development of an 8 tonne class hybrid hydraulic excavator SK80H. *Kobelco technology review*, *31*, 6-11.
[26] Wang, M. & Larish, C. (2015). Energy recovery system for excavators. *Fluid Power Innovation & Research Conference.*
[27] Joo, C. & Stangl, M. (2016). Application of Power Regenerative Boom system to excavator. *10th International Fluid Power Conference, Dresden*, 175-184.
[28] Li, W., Cao, B., Zhu, Z., & Chen, G. (2014). A novel energy recovery system for parallel hybrid hydraulic excavator. *Hindawi Publishing Corporation, Scientific World Journal,* Article ID 184909, 1-14. https://doi.org/10.1155/2014/184909
[29] Linjama, M., Huova, M., Pietola, M., Juhala, J., & Huhtala, K. (2015). Hydraulic hybrid actuator: theoretical aspects and solution alternatives. *The Fourteenth Scandinavian International Conference on Fluid Power.*
[30] Jianqi, L. (1992). An Energy-Saving Device Applied to the Swing System of Hydraulic Excavator. *International Fluid Power Exposition and Technical Conference*.
[31] Jovanović, V. (2018). *A contribution to the synthesis of the slewing platform drive mechanism of hydraulic excavators*. PhD dissertation, (in Serbian), University of Niš, Faculty of Mechanical Engineering.
[32] Mitrev, R., Janošević, D., & Marinković, D. (2017). Dynamical modelling of hydraulic excavator considered as a multibody system. *Tehnicki Vjesnik*, *24*(2), 327-338. https://doi.org/10.17559/TV-20151215150306
[33] Catalog Rothe Erde, *Slewing Bearings*, GmbH D-44137 Dortmund.
[34] Catalog INA, *Slewing Bearings*, Schaeffler Technologies AG & Co. KG Herzogenaurach, Germany.
[35] Jovanović, V., Janošević, D., & Petrović, N. (2014). Analysis of slewing bearing load of a rotating platform drive in hydraulic excavators. *Tehnicki Vjesnik*, *21*(2), 263-270.
[36] Mitrev, R. & Marinković, D. (2019). Numerical study of the hydraulic excavator overturning stability during performing lifting operations. *Advances in Mechanical Engineering*, *11*(5), 1-14. https://doi.org/10.1177/1687814019841779
[37] Janošević, D., Pavlović, J., Jovanović, V., & Petrović, G. (2018). A numerical and experimental analysis of the dynamic stability of hydraulic excavators. *Facta Universitatis-Series Mechanical Engineering*, *16*(2), 157-170. https://doi.org/10.22190/FUME180404015J
[38] Yuan, Y., Ren, J., Wang, Z., & Mu, X. (2022). Dynamic analysis of the rigid-flexible excavator mechanism based on virtual prototype. *Facta Universitatis, Series: Mechanical Engineering*. https://doi.org/10.22190/FUME211028008Y
[39] Catalog Rothe Erde, *Slewing Bearings*, GmbH D-44137 Dortmund.
[40] Liebherr-France SAS. (2014). Retrieved from http://www.coastlinecd.com/pdf/LiebherrMaterialHandlerRSeries/R974CCrawlerExcavator.pdf

Contact information:

Vesna JOVANOVIĆ, Assistant Professor
University of Niš,
Mechanical Engineering Faculty
Aleksandra Medvedeva 14, 18000 Niš, Serbia
E-mail: vesna.jovanovic@masfak.ni.ac.rs

Dragan MARINKOVIĆ, Full Professor
(Corresponding author)
1) University of Niš, Mechanical Engineering Faculty,
Aleksandra Medvedeva 14, 18000 Niš, Serbia
2) Technical University Berlin, Institute of Mechanics,
17. Juni 135, 10623 Berlin, Germany
E-mail: Dragan.Marinkovic@TU-Berlin.de

Dragoslav JANOŠEVIĆ, Full Professor, retired
University of Niš,
Mechanical Engineering Faculty,
Aleksandra Medvedeva 14, 18000 Niš, Serbia
E-mail: dragoslav.janosevic@masfak.ni.ac.rs

Nikola PETROVIĆ, Assistant Professor
University of Niš,
Mechanical Engineering Faculty,
Aleksandra Medvedeva 14, 18000 Niš, Serbia
E-mail: nikola.petrovic@masfak.ni.ac.rs